

Cold collisions of ground-state calcium atoms in a laser field: A theoretical study

Béatrice Bussery-Honvault and Jean-Michel Launay

Laboratoire PALMS, UMR 6627 du CNRS, Université de Rennes 1, Campus de Beaulieu, 35042 Rennes Cedex, France

Robert Moszynski*

Department of Chemistry, University of Warsaw, Pasteura 1, 02-093 Warsaw, Poland

(Received 12 March 2003; published 23 September 2003)

State-of-the-art *ab initio* techniques have been applied to compute the potential-energy curves for the ground $X\ ^1\Sigma_g^+$ and excited ${}^1\Pi_g(4s3d)$ states of the calcium dimer in the Born-Oppenheimer approximation. The weakly bound ground state was calculated by symmetry-adapted perturbation theory, while the strongly bound excited state was computed using a combination of the linear-response theory within the coupled-cluster singles and doubles framework for the core-valence electronic correlation and of the full configuration interaction for the valence-valence correlation. The ground-state potential has been corrected by considering the relativistic terms resulting from the first-order many-electron Breit theory, and the retardation corrections. The magnetic electronic transition dipole moment governing the ${}^1\Pi_g \leftarrow {}^1\Sigma_g^+$ transitions has been obtained as the first residue of the polarization propagator computed with the coupled-cluster method restricted to single and double excitations. The computed energies and transition moments have been analytically fitted and used in the dynamical calculations of the rovibrational energy levels, ground-state scattering length, photoassociation intensities at ultralow temperatures, and spontaneous emission coefficients from the ${}^1\Pi_g(4s3d)$ to the $X\ ^1\Sigma_g^+$ state. The spectroscopic constants of the theoretical ground-state potential are in a good agreement with the experimental values derived from the Fourier-transform spectra [O. Allard *et al.*, *Eur. Phys. J. D* (to be published)]. The theoretical *s*-wave scattering length for the ground state is $a=44$ bohrs, suggesting that it should be possible to obtain a stable Bose-Einstein condensate of calcium atoms. Finally, the computed photoassociation intensities and spontaneous emission coefficients suggest that it should be possible to obtain cold calcium molecules by photoassociation of cold atoms to the first ${}^1\Pi_g$ state followed by a spontaneous emission to the ground state.

DOI: 10.1103/PhysRevA.68.032718

PACS number(s): 34.20.Cf, 34.50.Rk, 32.80.Pj

I. INTRODUCTION

Recent developments in laser cooling and trapping techniques have opened the possibility of studying collisional dynamics at ultralow temperatures. Atomic Bose-Einstein condensates [1] are of crucial importance in this respect since investigations of the collisions between ultracold atoms in the presence of a weak laser field lead to precision measurements of the atomic properties and interactions. Such collisions may also lead to the formation of ultracold molecules that can be used in high-resolution spectroscopic experiments to study inelastic and reactive processes at very low temperatures, interatomic interactions at very large distances where the relativistic and QED effects are important, or the thermodynamic properties of the quantum condensates of dilute, weakly interacting atoms [2].

Until recently most of the experiments concentrated on the alkali-metal atoms (see Ref. [2] for a review). However, in a recent series of papers [3–7] it was shown that it is possible to trap and cool alkali-earth metal atoms, such as magnesium [3], calcium [4,5], and strontium [4,6,7]. Photoassociation spectra involving cold strontium [8] and calcium [9] atoms were also reported for the first time. On the theoretical side, studies of the cold collisions between alkali-

earth metal atoms are scarce [10–12] and restricted to magnesium atoms. It is worth noting here that the alkali-earth metal atoms have nondegenerate ground states with zero nuclear spin, so the analysis of the spectra is greatly simplified, compared to alkali-metal atoms.

The spectrum of the calcium dimer from cold calcium atoms observed in the photoassociation experiment of Ref. [9] showed regular vibrational series corresponding to the $B\ ^1\Sigma_u^+$ state, but the efficiency of the spontaneous emission to the bound vibrational levels of the ground $X\ ^1\Sigma_g^+$ state was very small. Since then new experimental schemes are being devised, in order to increase the efficiency of production of cold calcium molecules. One possible scheme concerns the photoassociative spectroscopy to the first ${}^1\Pi_g(4s3d)$ state [13]. The first aim of the present paper is to report on a theoretical investigation of the production of cold Ca_2 molecules by photoassociation to the $(1)\ ^1\Pi_g$ state followed by a spontaneous emission to the ground state. For this purpose, we performed high-accuracy *ab initio* calculations of the ground state and $(1)\ ^1\Pi_g$ state potential-energy curves, transition moment governing the $(1)\ ^1\Pi_g \leftarrow X\ ^1\Sigma_g^+$ transitions, photoassociation intensities from the vibrational continuum of the ground electronic state to the bound vibrational levels of the $(1)\ ^1\Pi_g$ state, and spontaneous emission coefficients back to the ground $X\ ^1\Sigma_g^+$ state.

Bose-Einstein condensate of calcium atoms has not been observed thus far. It is well known that the existence of a

*Corresponding author.

Email address: rmoszyns@chem.uw.edu.pl

stable condensate depends on the sign of the s -wave scattering length [1]. This quantity is not easily accessible to experiments since it depends critically on the number of bound vibrational states, on the position of the last bound state, and on the very long-range tail of the potential-energy curve. A reliable theoretical determination of the s -wave scattering length requires the knowledge of an accurate potential-energy curve, possibly including the relativistic and QED effects. Accurate calculation of the scattering length for the calcium dimer is the second aim of our paper. Present calculation of the ground-state potential-energy curve includes the relativistic and QED terms, so we also study the effect of these “exotic” contributions to the potential on the scattering length.

The calcium molecule is a very interesting system in its own. Due to the equal number of bonding and antibonding electrons, Ca_2 does not form a typical chemical bond. However, the dissociation energy of the order of 1000 cm^{-1} is not typical of van der Waals complexes bound by dispersion forces, but rather of hydrogen-bonded systems such as the water dimer. Our calculations on the ground state of Ca_2 employed the symmetry-adapted perturbation theory of intermolecular forces, so the potential energy was obtained in terms of physical contributions such as the electrostatics, induction, dispersion, and exchange. Thus, in the present paper we will be able to shed some light on the origins of the bonding in Ca_2 . Surprisingly, only a few *ab initio* calculations on the calcium dimer have been reported in the literature [14–17]. Most of them are at least ten years old, and thus not very accurate for the present day standards, while the most recent work of Mirick *et al.* [17] employed the density-functional theory. However, the results reported in Ref. [17] are not expected to be very accurate, since all density functionals available in the literature do not reproduce the correct R^{-6} behavior of the interatomic potentials. See Ref. [18] for the discussion of this point, and Ref. [19] for numerical examples for various weakly bound van der Waals complexes. not very well suited for molecules with strong dispersion interactions. In addition, several papers appeared [20–24] reporting calculations of the long-range dispersion coefficients by *ab initio* methods or using semiempirical approaches.

The calcium dimer was the subject of numerous high-resolution spectroscopic studies in the gas phase [25–34] and in rare gas matrices [35–39]. Until recently, the dissociation energy of the ground state of Ca_2 could only be estimated from the Rydberg-Klein-Rees (RKR) inversion of the spectroscopic data for the $B^1\Sigma_u^+ \leftarrow X^1\Sigma_g^+$ transitions [28]. In two recent papers, Tiemann and co-workers [33,34] reported a much more elaborate study of Ca_2 by measuring the $B^1\Sigma_u^+ \leftarrow X^1\Sigma_g^+$ transitions covering over 99.8% of the well depth. However, the long-range part of the potential is not easily accessible to spectroscopic experiments, although it is crucial for an accurate determination of the scattering length. In any case, comparison between the present theoretical predictions and the most recent high-resolution spectroscopic data [33,34] will enable us to judge critically the accuracy of the present calculations.

The plan of this paper is as follows. In Sec. II, we intro-

duce the theoretical models used in our calculations. We start this section with a brief description of the methods used in *ab initio* calculations of the Born-Oppenheimer potential-energy curves and transition moment for Ca_2 . We discuss the relativistic effects and the QED retardation of the relativistic potential. We also give details of the fits of the computed points to some analytical expressions for the potentials and the transition moment. The choice of these expressions and methods of fixing some asymptotic coefficients at their *ab initio* values are briefly addressed. The remaining part of this section is devoted to the second step of the Born-Oppenheimer approximation, i.e., to dynamical calculations of the scattering length, photoassociation intensities, and spontaneous emission coefficients. Numerical results are presented and discussed in Sec. III. We start this section with the discussion of the ground state of the calcium dimer. We discuss the origins of the bonding in Ca_2 , and compare the theoretical ground-state spectroscopic constants with those derived from high-resolution experiments [28,33,34]. Once the accuracy of the theoretical ground state is established, we turn to the problem of producing cold calcium molecules. We present the photoassociation spectrum, and suggest an efficient scheme leading to cold Ca_2 . Finally, in Sec. IV we conclude our paper.

II. METHODS OF CALCULATIONS

A. Ground-state potential

It follows from the naive molecular-orbital theory that the calcium dimer in the ground state should be considered as a van der Waals molecule since the molecular configuration has an equal number of the bonding and antibonding electrons. No regular chemical bond is expected, except for a weak dispersion attraction and exchange repulsion. Therefore in the present paper, we report on calculations of the ground-state potential-energy curve by symmetry-adapted perturbation theory (SAPT) of intermolecular forces [40,41]. We follow the computational approach introduced and tested in previous papers on van der Waals molecules (see, e.g., Ref. [42] for a recent paper, and Refs. [40,41] for the reviews of the SAPT approach). The ground-state potential $V_g^{\Sigma_g^+}$ was computed from the following expression:

$$V_g^{\Sigma_g^+} = E_{\text{elst}}^{(1)} + E_{\text{ind}}^{(2)} + E_{\text{disp}}^{(2)} + E_{\text{exch}}, \quad (1)$$

where the consecutive terms on the right-hand side (rhs) of Eq. (1) denote the electrostatic, induction, dispersion, and exchange energies, respectively. Note that no multipole approximation of the intermolecular interaction operator has been used, so the electrostatic and induction terms do not vanish, but represent pure penetration (charge-overlap) effects. Furthermore, the dispersion contribution is not solely represented by the asymptotic expansion in terms of the van der Waals constants, but it also includes important (short-range) charge-overlap effects. The exchange contribution can further be decomposed as follows:

$$E_{\text{exch}} = E_{\text{exch}}^{(1)} + E_{\text{exch-ind}}^{(2)} + E_{\text{exch-def}}^{(2)} + E_{\text{exch-disp}}^{(2)}. \quad (2)$$

Here, $E_{\text{exch}}^{(1)}$ is the first-order exchange energy, while $E_{\text{exch-ind}}^{(2)}$, $E_{\text{exch-def}}^{(2)}$, and $E_{\text{exch-disp}}^{(2)}$ denote the exchange-induction, exchange-deformation, and exchange-dispersion terms. The contributions appearing on the rhs of Eqs. (1) and (2) have been evaluated using the many-body techniques developed in Refs. [43–50]. The exchange-deformation energy was computed directly from the supermolecule Hartree-Fock interaction energy. The computational scheme for the Ca · · · Ca interactions was the same as in our previous works (see, for instance, Refs. [42,51]). The SAPT calculations were done with the program SAPT [52].

The ground state of the calcium atom is a nondegenerate 1S state, so the potential depends solely on the interatomic distance R . Calculations have been performed for 15 interatomic distances ranging from $R=3$ to 15 bohrs. For the ground-state potential, we chose a $[9s7p3d2f2g]$ basis set. The $[9s7p2d]$ part of this basis was optimized for the ground-state polarizability of the calcium atom [53], while the exponents of the additional polarization functions of d , f , and g symmetry were chosen to minimize the dispersion contribution to the ground-state energy of the Ca dimer. In addition, the leading-order dispersion term has been recomputed in the $[9s7p3d2f2g]$ basis supplemented with a set of $[3s3p2d]$ bond functions. The SAPT energies were always computed with the dimer basis set.

The computed points were fitted to the following analytic expression:

$$V_g^{\Sigma^+}(R) = (A_1 + B_1 R)e^{-\alpha_1 R} + (A_2 + B_2 R)e^{-\alpha_2 R} - \sum_{n=3}^5 \frac{C_{2n}}{R^{2n}} f_{2n}(\beta, R), \quad (3)$$

where $\{A_i\}_{i=1}^2$, $\{B_i\}_{i=1}^2$, $\{\alpha_i\}_{i=1}^2$, and β were adjusted to the computed points, while the long-range dispersion coefficients C_n were not fitted, but computed in the same basis set and at the same level of the theory as the nonexpanded dispersion energy [54]. This means that the computed C_n coefficients define the large R asymptotic behavior of the computed SAPT dispersion energy $E_{\text{disp}}^{(2)}$:

$$E_{\text{disp}}^{(2)} \sim - \sum_{n=3}^5 \frac{C_{2n}}{R^{2n}}. \quad (4)$$

The damping function $f_n(\beta, R)$ that ensures a correct behavior of the potential in the repulsive region was taken in the Tang-Toennies form [55]:

$$f_n(\beta, R) = 1 - e^{-\beta R} \sum_{k=0}^n \frac{(\beta R)^k}{k!}. \quad (5)$$

The long-range coefficients were computed with the program POLCOR [56,57].

B. Relativistic corrections to the ground-state potential

The calcium dimer is a relatively light system, so we expect that the relativistic contribution to the ground-state po-

tential can be obtained from the many-electron Breit-Pauli Hamiltonian [58] valid to the first order in α^2 , where α is the fine-structure constant. It follows from the work of Sadlej *et al.* [53] that the relativistic correction to the dipole polarizability of the calcium atom represents ca. 1.3% of the non-relativistic value. Since the leading contribution to the interaction potential, the dispersion energy, depends directly on the atomic polarizability, we expect a similar effect of the relativistic terms on the Ca_2 potential. Consequently, the first-order Breit-Pauli approximation should work well in our case. For a closed-shell system, the Breit-Pauli Hamiltonian reads [59]

$$H_{\text{B-P}} = H_1 + H_2 + H_3 + H_4, \quad (6)$$

$$H_1 = -\frac{\alpha^2}{8} \sum_{i=1}^N \mathbf{p}_i^4, \quad H_2 = \frac{\pi \alpha^2}{2} \sum_{\gamma} \sum_{i=1}^N Z_{\gamma} \delta(\mathbf{r}_{\gamma i}),$$

$$H_3 = -\pi \alpha^2 \sum_{i>j=1}^N \delta(\mathbf{r}_i - \mathbf{r}_j), \quad (7)$$

$$H_4 = -\frac{\alpha^2}{2} \sum_{i>j=1}^N \frac{1}{\mathbf{r}_{ij}^3} [(\mathbf{r}_i - \mathbf{r}_j)^2 \mathbf{p}_i \cdot \mathbf{p}_j + (\mathbf{r}_i - \mathbf{r}_j) \cdot [(\mathbf{r}_i - \mathbf{r}_j) \cdot \mathbf{p}_i] \mathbf{p}_j], \quad (8)$$

where \mathbf{r}_i and \mathbf{p}_i denote the position and momentum operators of the i th electron, $\mathbf{r}_{\gamma i}$ is the position of the i th electron with the respect to the nucleus γ , Z_{γ} represents the charge of the nucleus γ , and N is the number of electrons. The Hamiltonian H_1 describes the so-called relativistic mass-velocity contribution. The terms H_2 and H_3 are often referred to as the one-electron and two-electron Darwin terms, respectively, while the last entry in Eq. (6), H_4 , describes the relativistic orbit-orbit interaction.

It follows from the work of Hirschfelder and Meath [59–61] that for the interaction of two closed-shell atoms the following long-range behavior of the relativistic contributions to the ground-state potential [denoted by $V_g^{\Sigma^+}(H_i)$] is expected:

$$V_g^{\Sigma^+}(H_1) \sim \frac{C_6^{H_1}}{R^6} + \dots, \quad V_g^{\Sigma^+}(H_2) \sim \frac{C_6^{H_2}}{R^6} + \dots, \quad (9)$$

$$V_g^{\Sigma^+}(H_4) \sim \frac{C_4^{H_4}}{R^4} + \frac{C_6^{H_4}}{R^6} + \dots. \quad (10)$$

The expressions for the long-range relativistic coefficients $C_6^{H_i}$ can be written in terms of the quadratic response functions involving two dipole operators and the relativistic operator H_1 or H_2 , and will be reported in a forthcoming paper [62]. As shown in Ref. [60], the leading asymptotic term $C_4^{H_4}/R^4$ of the orbit-orbit contribution, $V_g^{\Sigma^+}(H_4)$, to the ground-state potential is implicitly included in the retardation effect of the dipole-dipole dispersion interaction (cf. Sec. II C). This means that if the retardation of the potential is

included, the C_4^H/R^4 term does not need to be considered. According to Ref. [59], the two-electron Darwin contribution $V_{\text{ret}}^{\Sigma_g^+}(H_3)$ vanishes exponentially with R , so we can treat the relativistic effects in Ca_2 within the following model Hamiltonian due to Cowan and Griffin [63]:

$$H_{\text{C-G}} = -\frac{\alpha^2}{8} \sum_{i=1}^N \mathbf{p}_i^4 + \frac{\pi\alpha^2}{2} \sum_{\gamma} \sum_{i=1}^N Z_{\gamma} \delta(\mathbf{r}_{\gamma i}), \quad (11)$$

i.e., approximate the relativistic contribution to the ground-state potential by the sum $V_{\text{ret}}^{\Sigma_g^+}(H_1) + V_{\text{ret}}^{\Sigma_g^+}(H_2)$. It is worth noting that the usefulness of the Cowan-Griffin model of the relativistic effects on the properties of atoms and molecules has been documented in several *ab initio* calculations (see Ref. [53] and references therein).

In practice, the relativistic contributions $V_{\text{ret}}^{\Sigma_g^+}(H_1)$ and $V_{\text{ret}}^{\Sigma_g^+}(H_2)$ were obtained from finite-field supermolecule calculations within the coupled-cluster theory restricted to single, double, and noniterative triple excitations [CCSD(T)] [64]:

$$V_{\text{ret}}^{\Sigma_g^+}(H_i) = \left(\frac{\partial}{\partial \lambda} [E_{\text{AB}}^{\text{CCSD(T)}}(\lambda) - E_{\text{A}}^{\text{CCSD(T)}}(\lambda) - E_{\text{B}}^{\text{CCSD(T)}}(\lambda)] \right)_{\lambda=0}, \quad (12)$$

where $E_X^{\text{CCSD(T)}}(\lambda)$ ($X=A, B$, or AB), denotes the CCSD(T) energy of the dimer AB computed with the Hamiltonian $H_X + \lambda H_i$. The derivative appearing in Eq. (12) was approximated by a three-point finite-difference formula. We have checked that $\lambda = 10^{-4}$ was sufficient to obtain stable results for all interatomic distances considered in the present paper.

C. Retardation of the relativistic ground-state potential

Some quantities appearing in our study of cold calcium atoms' collisions, such as the scattering length or the positions of high-lying vibrational levels of the ground electronic state, are sensitive to the wave function at distances comparable to the characteristic atomic length $\lambda_0 = (\alpha\Delta E)^{-1}$, where ΔE is the excitation energy from the ground to the first excited atomic state. At these distances the nonrelativistic potential no longer behaves as R^{-6} , but it should be corrected for the retardation effects according to the Casimir-Polder formula [65]:

$$V_{\text{ret}}^{\Sigma_g^+} = -\frac{1}{\pi R^6} \int_0^{\infty} \alpha_1^2(i\omega) \exp(-2\omega R/c) P(\omega R/c) d\omega, \quad (13)$$

where $\alpha_1(i\omega)$ denotes the dynamic dipole polarizability of the atom at an imaginary frequency $i\omega$, $c = e^2/\hbar\alpha$ is the speed of light, and

$$P(x) = x^4 + 2x^3 + 5x^2 + 6x + 3. \quad (14)$$

The retardation effects also affect the relativistic potential. When the retardation is taken into account, the relativistic terms $V_{\text{ret}}^{\Sigma_g^+}(H_i)$, $i=1,2$, become [62]:

$$V_{\text{ret}}^{\Sigma_g^+}(H_i) = \frac{2}{\pi R^6} \int_{-\infty}^{\infty} \beta^{H_i}(i\omega, 0) \alpha_1(i\omega) \times \exp(-2\omega R/c) P(\omega R/c) d\omega, \quad (15)$$

where $\beta^{H_i}(i\omega, 0)$ denotes the quadratic response function with two dipole operators and one relativistic operator H_1 or H_2 , and can be related to the change in the atomic dynamic polarizability at an imaginary frequency $i\omega$ due to the relativistic term H_i . A detailed derivation of Eq. (15) will be reported elsewhere [62]; here suffice it to say that it gives a correct asymptotic behavior of the relativistic potential for distances smaller and much larger than the characteristic atomic length λ_0 . In the present paper, the retardation effects on the nonrelativistic, mass-velocity, and one-electron Darwin terms were explicitly taken into account.

D. Excited-state potential

The first ${}^1\Pi_g$ state of the calcium dimer dissociating into $\text{Ca}({}^1S) + \text{Ca}({}^1D)$ is expected to be strongly bound. Therefore, the corresponding potential-energy curve V^{Π_g} has been obtained by a supermolecule method. In order to obtain accurate results, we decided to employ a hybrid method. We treated the core-valence electronic correlation (with a frozen core of 10 electrons) by the linear-response theory within the coupled-cluster singles and doubles (LRCCSD) framework [66], while the valence-valence contribution was obtained from the full configuration-interaction (FCI) calculations. Thus, V^{Π_g} was constructed according to the formula:

$$V^{\Pi_g} = V_{\text{c-c}}^{\Pi_g} + V_{\text{c-v}}^{\Pi_g} + V_{\text{v-v}}^{\Pi_g}. \quad (16)$$

The core-core ($V_{\text{c-c}}^{\Pi_g}$) and core-valence ($V_{\text{c-v}}^{\Pi_g}$) contributions to the potential were obtained from the linear-response CCSD calculations:

$$V_{\text{c-c}}^{\Pi_g} + V_{\text{c-v}}^{\Pi_g} = [E_{\text{AB}}^{\text{LRCCSD}}(20e) - E_{\text{A}}^{\text{LRCCSD}}(10e) - E_{\text{B}}^{\text{LRCCSD}}(10e)] - [E_{\text{AB}}^{\text{LRCCSD}}(4e) - E_{\text{A}}^{\text{LRCCSD}}(2e) - E_{\text{B}}^{\text{LRCCSD}}(2e)], \quad (17)$$

where $E_{\text{AB}}^{\text{LRCCSD}}(Ne)$ denotes the energy of the dimer computed using the LRCCSD method with N electrons correlated, and similar definitions apply to atomic energies appearing in Eq. (17), except that for atoms where only half of the electrons are in the valence shell. The valence-valence correlation contribution was computed from the expression

$$V_{\text{v-v}}^{\Pi_g} = [E_{\text{AB}}^{\text{FCI}}(4e) - E_{\text{A}}^{\text{FCI}}(2e) - E_{\text{B}}^{\text{FCI}}(2e)], \quad (18)$$

where the energies appearing on rhs denote the FCI energies of the dimer AB and of the atoms A and B , with four and two electrons correlated, respectively. In the excited-state calculations, the relativistic and retardation corrections are not as

crucial as for the ground state, so in the present calculations they were neglected. The LRCCSD calculations were performed with the DALTON program [67], while the FCI calculations employed the MOLCAS code [64].

The $(1) {}^1\Pi_g$ potential-energy curve was computed for 15 distances R ranging from 4 to 15 bohrs. For the excited-state potential, we chose the $[9s7p5d2f2g]$ basis set. The $[9s7p]$ part of this basis and the exponents of the f and g functions were the same as for the ground state, while the exponents of the five d functions were optimized to reproduce the atomic 1S - 1D splitting at the LRCCSD level. The full basis of the dimer was used in all supermolecule calculations for the excited state, and so the Boys and Bernardi scheme was used to correct for basis-set superposition error [68].

The computed energies were fitted to the following analytic expression:

$$V^{\Pi_g}(R) = (A_1 + B_1 R)e^{-\alpha_1 R} + (A_2 + B_2 R)e^{-\alpha_2 R} + \frac{C_5}{R^5} f_5(\beta, R) - \sum_{n=3}^5 \frac{C_{2n}}{R^{2n}} f_{2n}(\beta, R), \quad (19)$$

where $\{A_i\}_{i=1}^2$, $\{B_i\}_{i=1}^2$, $\{\alpha_i\}_{i=1}^2$, β , and $\{C_{2n}\}_{n=3}^5$ were adjusted to the computed points, while the leading long-range coefficient C_5 describing the first-order resonant interaction [61] of $\text{Ca}({}^1S)$ and $\text{Ca}({}^1D)$ was not fitted, but computed in the same basis set and at the same level of the theory as that of the total excited-state potential. The C_5 coefficient was obtained from the expression

$$C_5 = -\frac{32\pi}{5} |\langle \Psi_{\text{Ca}}({}^1S) | Q_2^1 | \Psi_{\text{Ca}}({}^1D) \rangle|^2, \quad (20)$$

where $\Psi_{\text{Ca}}({}^1S)$ and $\Psi_{\text{Ca}}({}^1D)$ denote the wave functions of the calcium atom in the 1S and 1D states, respectively, and Q_2^1 is the atomic quadrupole moment operator. It follows from Eq. (20) that the C_5 coefficient is negative, so no barrier or long-range minimum is expected on the $(1) {}^1\Pi_g$ potential-energy curve. Note that at large distances the LRCCSD and FCI contributions to the first-order resonant interaction energy are identical, so the matrix element of Eq. (20), defining the asymptotic behavior of Eq. (16), can be computed at the LRCCSD level as the first residue of an appropriate propagator. To prove this point, we note that at large R the four-electron CCSD wave function behaves like [40]

$$\Psi_{\text{AB}}^{\text{CCSD}}(4e) = \mathcal{A} \Psi_{\text{A}}^{\text{CCSD}}(2e) \Psi_{\text{B}}^{\text{CCSD}}(2e) + O(R^{-3}), \quad (21)$$

where \mathcal{A} is the antisymmetrizer ensuring the correct permutational symmetry. Similarly, the four-electron FCI wave function becomes at large R :

$$\Psi_{\text{AB}}^{\text{FCI}}(4e) = \mathcal{A} \Psi_{\text{A}}^{\text{FCI}}(2e) \Psi_{\text{B}}^{\text{FCI}}(2e) + O(R^{-3}). \quad (22)$$

Since for two-electron systems the CCSD and FCI wave functions are equal, it follows directly from Eqs. (21) and (22) that they do not contribute to C_5 .

The transitions from the ground $X {}^1\Sigma_g^+$ state to the $(1) {}^1\Pi_g$ are not electric dipole allowed. However, these transitions are allowed by the magnetic transition dipole moment (the so-called $M1$ transitions) [69]:

$$M = -\frac{e}{2m} \langle \Psi_{\text{AB}}({}^1\Sigma_g^+) | L_x | \Psi_{\text{AB}}({}^1\Pi_g) \rangle, \quad (23)$$

where $\Psi_{\text{AB}}({}^1\Sigma_g^+)$ and $\Psi_{\text{AB}}({}^1\Pi_g)$ denote the wave functions for the ${}^1\Sigma_g^+$ and ${}^1\Pi_g$ states, respectively, and L_x is the x component of the angular-momentum operator for the Ca dimer. In the present calculations, the magnetic transition dipole moment M was computed as the first residue of the LRCCSD linear-response function with two L_x operators [66], used in the computations of the excited-state potential. The DALTON program [67] was used in these calculations.

The transition moment was evaluated for the same distances as the excited-state potential. The computed values were fitted to the following expression:

$$M(R) = (A_1 + B_1 R)e^{-\alpha_1 R} + (A_2 + B_2 R)e^{-\alpha_2 R} + \sum_{n=5}^8 \frac{C_n}{R^n} f_n(\beta, R), \quad (24)$$

where $\{A_i\}_{i=1}^2$, $\{B_i\}_{i=1}^2$, $\{\alpha_i\}_{i=1}^2$, β , and $\{C_n\}_{n=5}^8$ are adjustable parameters. Note that the long-range coefficients governing the asymptotic behavior of the magnetic transition dipole moment were not computed independently, but rather fitted to the numerical values. However, the analytic form of the R^{-1} expansion follows directly from the multipole expansion of the ${}^1\Sigma_g^+$ and $(1) {}^1\Pi_g$ wave functions of the dimer.

To end this section, we wish to say that the ${}^1\Sigma_g^+$ and ${}^1\Pi_g$ states are also connected by an electric quadrupole transition (the so-called $E2$ transition). However, the $E2$ transitions are usually much weaker than $M1$ [70], so in the present paper they were neglected.

E. s -wave scattering length

As discussed in the Introduction, the s -wave scattering length for the ground-state potential of the calcium dimer is the crucial quantity [1] that determines the possibilities of obtaining stable Bose-Einstein condensates of calcium atoms. To introduce the s -wave scattering length, let us consider the scattering of two calcium atoms for $J=0$ at an energy $E = \hbar^2 k^2 / 2\mu$, where μ is the reduced mass of the collisional complex. The radial part of the nuclear wave function satisfies the following equation:

$$\left(\frac{d^2}{dR^2} - \frac{2\mu}{\hbar^2} V^{\Sigma_g^+}(R) + k^2 \right) \psi(R; k) = 0. \quad (25)$$

At large distances R , the scattering wave function $\psi(R; k)$ behaves like

$$\psi(R; k) \rightarrow \sin(kR) + \tan \eta(k) \cos(kR), \quad (26)$$

where $\eta(k)$ is the phase shift. The phase shift defines formally the s -wave scattering length by the expression

$$a = \lim_{k \rightarrow 0} \frac{-\tan \eta(k)}{k}. \quad (27)$$

In practical calculations the formal definition of Eq. (27) is not convenient. Instead one can compute a from the analysis of the wave function at zero energy. It follows directly from Eq. (25) that at sufficiently large distances $R > R_0$ [where the potential $V_{\Sigma_g^+}(R)$ is zero], the wave function $\psi(R;0)$ behaves like

$$\psi(R;0) \sim a_1 R + a_2. \quad (28)$$

Once linear function (28) is obtained for $\psi(R;0)$, the scattering length is simply given by $-a_2/a_1$. Note that this simple computational approach to the scattering length requires the solution of the Schrödinger equation at very large distances, where the wave function $\Psi(R;0)$ can effectively be approximated by Eq. (28).

F. Photoassociation absorption to the excited state and spontaneous emission to the ground state

The production of ultracold molecules by photoassociation spectroscopy is conducted according to the following pumping scheme. We start with the absorption of a photon by the gas of ultracold ^{40}Ca atoms. This process will lead to a transition from the vibrational continuum of the ground electronic state to an excited vibrational level v' of the $(1)^1\Pi_g$ state of Ca_2 . The corresponding absorption coefficient $K(\nu, T)$ at a frequency ν is given by [71,72]

$$K(\nu, T) = \frac{8\pi^3 \nu n^2}{3c^3 Q_T} \frac{1}{4\pi\epsilon_0} \sum_{v'} \exp[-\Delta_{v'}(\nu)/k_B T] \\ \times \sum_{J''} g_{J''}[(J''+1)] |\langle \psi_{v', J''+1} | M | \Psi_{E, J''} \rangle|^2 \\ + J'' |\langle \psi_{v', J''-1} | M | \Psi_{E, J''} \rangle|^2, \quad (29)$$

where n is the gas number density, T is the temperature, k_B is the Boltzmann constant, $Q_T = (\mu k_B T / 2\pi\hbar^2)^{3/2}$ is the translational partition function, $g_{J''}$ is the spin statistical weight depending on the nuclear spin (equal to 1 for ^{40}Ca), and $E = \Delta_{v'}(\nu)$ is the detuning relative to the position of the level v' , i.e., $\Delta_{v'} = E_{v'} - h\nu$. Equation (29) is strictly valid for red detunings, i.e., for $h\nu - E_{v'}$. For blue detuning frequencies, $\Delta_{v'}$ should be defined as $h\nu - E_{v'}$. Note that for the $1^1\Sigma_g^+ \leftarrow 1^1\Pi_g$ transitions the selection rule $J' = J'' \pm 1$ applies [69], so the wave functions of the upper levels $\psi_{v', J'}$ appear with the J' labels equal to $J'' \pm 1$. The wave functions in Eq. (29) are solutions of the Schrödinger equations:

$$\left(\frac{d^2}{dR^2} - \frac{2\mu}{\hbar^2} V_{\Sigma_g^+}(R) - \frac{J''(J''+1)}{R^2} + \frac{2\mu E}{\hbar^2} \right) \Psi_{E, J''}(R) = 0, \quad (30)$$

$$\left(\frac{d^2}{dR^2} - \frac{2\mu}{\hbar^2} V_{\Pi_g}(R) - \frac{J'(J'+1)}{R^2} + \frac{2\mu E_{v', J'}}{\hbar^2} \right) \psi_{v', J'}(R) = 0, \quad (31)$$

subject to the following normalization conditions:

$$\int_0^\infty \Psi_{E_1, J'}^*(R) \Psi_{E_2, J'}(R) dR = \delta(E_1 - E_2), \quad (32)$$

$$\int_0^\infty \psi_{v_1', J'}^*(R) \psi_{v_2', J'}(R) dR = \delta_{v_1' v_2'}. \quad (33)$$

The absorption process described above is followed by a spontaneous decay into the vibrational continuum of the ground electronic state. However, a fraction of the decay ends in the highest vibrational levels of the ground $X^1\Sigma_g^+$ state. The discrete transitions from the bound vibrational levels of the excited electronic state to bound vibrational levels of the ground electronic state will lead to the formation of cold molecules. This process can be characterized by the spontaneous emission coefficient $A_{v', J', v'', J''}$:

$$A_{v', J', v'', J''} = \frac{4}{3\hbar^4 c^5} \frac{1}{4\pi\epsilon_0} H_{J'} (E_{v'', J''} - E_{v', J'})^3 \\ \times |\langle \psi_{v', J'} | M | \psi_{v'', J''} \rangle|^2, \quad (34)$$

where the Hönl-London factor $H_{J'}$ is equal to $(J'+1)/(2J'+1)$ for the P branch and to $J'/(2J'+1)$ for the R branch. For the calcium dimer the spacing of the rotational levels is very small, so the use of Eq. (34) is not very practical. However, assuming that the energies and the matrix elements appearing in Eq. (34) are J independent, we get the following approximate expression [73]:

$$A_{v', v''} = \frac{4}{3\hbar^4 c^5} \frac{1}{4\pi\epsilon_0} (E_{v''0} - E_{v'0})^3 |\langle \psi_{v'0} | M | \psi_{v''0} \rangle|^2. \quad (35)$$

As discussed above the spontaneous emission mostly ends in the vibrational continuum of the electronic ground state. To estimate the contribution of the continuum states to the total transition probability, we assume that the relative transition probabilities of the spontaneous decay from the excited level v' to any ground level v'' are approximately equal to the Franck-Condon factors:

$$p_{v'} = \sum_{v''} |\langle \psi_{v'0} | \psi_{v''0} \rangle|^2, \quad (36)$$

where the summation over v'' is restricted to bound vibrational levels of the electronic ground state. Within this model, the probability that the transition from the level v' terminates in the continuum is simply given by $q_{v'} = 1 - p_{v'}$.

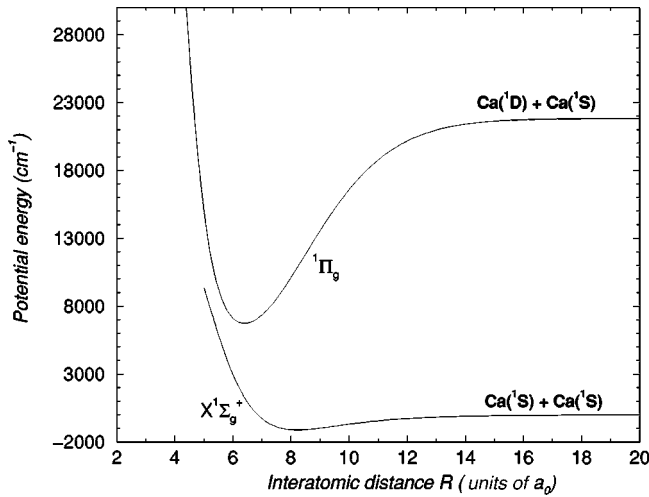


FIG. 1. Potential-energy curves for the $X^1\Sigma_g^+$ and (1) $^1\Pi_g(4s3d)$ states of Ca_2 . Energies are in cm^{-1} and distances in bohrs.

III. NUMERICAL RESULTS AND DISCUSSION

A. Potential-energy curve and spectroscopic characteristics of the $X^1\Sigma_g^+$ state of Ca_2

We start the discussion of our results with a closer look at the ground state of the calcium dimer. The potential-energy curve for the $X^1\Sigma_g^+$ state is presented in Fig. 1, while the most important spectroscopic characteristics of the Ca_2 ground state are gathered in Table I. An inspection of Table I shows that the calcium dimer is a relatively weakly bound diatomic molecule. The binding energy (1134 cm^{-1}) is not characteristic of molecules bound by strong chemical forces, but rather by weak van der Waals forces. It is worth noting that the relativistic effects, although small (of the order of 1.5% of the nonrelativistic well depth), change the binding energy in the right direction ($D_e = 1113 \text{ cm}^{-1}$), while the retardation of the dipole-dipole dispersion term does not contribute to the significant figures reported in Table I.

It is interesting to note that the present calculation of the binding energy of Ca_2 is by far much more accurate than all

previous calculations reported in the literature. Indeed, our binding energy of 1113 cm^{-1} is only 1% lower than the value determined from the analysis of the high-resolution spectra [33,34]. The early density-functional calculation of Jones [14] overestimated the well depth by as much as 46%. More recent calculations reduced this error considerably, but still the result of Dyall and McLean [16] is 12% off the experimental value, while the most recent density-functional study [17] gives a binding energy which overestimates the experimental value by $\approx 5\text{--}45\%$, depending on the functional used in the calculations.

Also reported in Table I are the spectroscopic data for the ground state of the calcium dimer derived from high-resolution experiments in the gas phase [28,33,34]. The theoretical dissociation energy ($D_0 = 1082 \text{ cm}^{-1}$) is in good agreement with the most recent experimental value ($D_0 = 1070 \text{ cm}^{-1}$) from Tiemann and co-workers [33], the difference between the computed and measured values being only 1.1%. Also our predicted number of bound vibrational states for $J=0$ agrees with the experiment, i.e., $N_v = 41$.

The dissociation energy of the ground-state calcium dimer was the subject of several high-resolution spectroscopic studies in the gas phase [28,33,34]. In 1980 Vidal [28] estimated the dissociation energy to be 1063 cm^{-1} by the RKR inversion of the spectroscopic data for the $A^1\Sigma_u^+ \leftarrow X^1\Sigma_g^+$ transitions. However, the number of vibrational states for $J=0$ extracted in Vidal's experiment, $N_v = 34$, was not sufficient to extrapolate the RKR potential-energy curve to the dissociation limit. Nevertheless, the potential-energy curve of Ref. [28], when extrapolated to large distances with an estimated long-range coefficient C_6 [28], gives the dissociation energy and the number of bound states much closer to the most recent experimental data (1067 cm^{-1} for D_0 and 40 for N_v).

As discussed in the Introduction, the SAPT method allows us to analyze the origins of the bonding in terms of some physically meaningful contributions, such as the electrostatic, induction, dispersion, and exchange terms. One could think that the calcium dimer is mostly bound by the Heitler-London energy, i.e., the sum of the electrostatic and first-order exchange energies, $E_{\text{elst}}^{(1)} + E_{\text{exch}}^{(1)}$, and by the dispersion energy $E_{\text{disp}}^{(2)}$. An inspection of Table II shows that the two contributions mentioned above are indeed dominant. How-

TABLE I. Spectroscopic characteristics of the ground- and excited-states potentials for the calcium dimer.

	R_e (bohrs)	D_e (cm^{-1})	D_0 (cm^{-1})	N_v	a (bohrs)
Ground state $X^1\Sigma_g^+$					
SAPT-nonrelativistic	8.2	1134	1103	41	-140.0
SAPT-relativistic	8.2	1113	1082	41	+46.0
SAPT-retarded	8.2	1113	1082	41	+44.0
RKR-Vidal [28]	8.1	1095	1063	34	-104.0
RKR-Vidal (extrapolated)	8.1	1098	1067	40	+53.0
Ref. [33]		1102	1069.88(9)	41	[+112, +850]
Ref. [34]		1102	1069.87(1)	41	[+250, +1000]
Excited state $^1\Pi_g(4s3d)$					
LRCCSD/FCI-nonrelativistic	6.4	15127	15048	157	

TABLE II. Components (in cm^{-1}) of the ground-state interaction potential of the calcium dimer at the minimum and in the attractive region.

	$R=8$ bohrs	$R=10$ bohrs	$R=12$ bohrs
$E_{\text{elst}}^{(1)} + E_{\text{exch}}^{(1)}$	2422.0	472.0	81.0
$E_{\text{ind}}^{(2)} + E_{\text{exch-ind}}^{(2)} + E_{\text{exch-def}}^{(2)}$	-1117.0	-308.0	-55.0
$E_{\text{disp}}^{(2)}$	-2898.0	-1021.0	-354.0
$E_{\text{exch-disp}}^{(2)}$	478.0	153.0	36.0
Total	-1115.0	-704.0	-292.0

ever, their sum is only slightly attractive, and underestimates the interaction energy by as much as $\approx 60\%$. The missing contributions come from the second-order induction, exchange-induction, and exchange dispersion terms. It is worth noting that the attractive dispersion energy is almost three times larger than the potential at the minimum, while the sum of the short-range contributions is two times larger than the absolute value of the potential at the minimum. At large distances the short-range contributions decay exponentially, while the dispersion term falls off as R^{-6} . Therefore, the balance between the attractive and repulsive contributions will change in the favor of the $E_{\text{disp}}^{(2)}$ term. This is already observed for $R=12$ bohrs. At this distance the dispersion contribution is dominant, while the short-range contributions represent (small) corrections. Obviously, at shorter distances the sum of the electrostatic, induction, and various exchange terms will be relatively more important than the dispersion energy.

Since the dispersion energy (including the relativistic corrections) determines the long-range behavior of the ground-state potential for Ca_2 , it is interesting to compare the long-range dispersion coefficients C_n computed in the present paper with other theoretical values [20–24], and with the values obtained by fitting the potential to the spectroscopic data [28,34]. This issue is of primary importance since, as will be shown in the following section, the s -wave scattering length is very sensitive to the value of the long-range dispersion coefficients. All the existing data are gathered in Table III. An inspection of this table shows that the most recent theoretical values agree with each other within a few percent. Indeed, the present nonrelativistic value of C_6 is only 2.3%

lower than the result of Mérawa *et al.* [23], while the present relativistic value of 2237 is in an excellent agreement with the relativistic result of Porsev and Derevianko [24], 2221 ± 15 . The agreement with the older data of Maeder and Kutzelnigg [20] and of Stanton [22] is worse, and the differences amount roughly to 10%. Standard and Certain [21] reported bounds to the long-range dispersion coefficients for Ca_2 . All the theoretical values for the C_6 coefficient reported in the literature are far from the lower bound reported in Ref. [21]. Hence, we conclude that these bounds are not reliable, at least for the C_6 coefficient of Ca_2 . The agreement between the present result and the recent C_6 coefficients derived from the experimental data of Tiemann and co-workers [34] by fitting the potential-energy curve to the observed spectroscopic transitions is not good. In fact our C_6 constant is in better agreement with the old estimate of Vidal [28] than with the newly fitted value from Ref. [34]. Given the excellent agreement between the most recent theoretical values (the present data and the data from Refs. [23,24]), we believe that the value of C_6 fitted to the experimental data [34] is a few percent too low. This may be partly due to the complete neglect of the short-range contributions to the potential at distances larger than 9.5 Å.

To the best of our knowledge, higher-order coefficients C_8 and C_{10} have been reported only in Refs. [20,21,33,34]. Our relativistic C_8 coefficient is well within the bounds reported both in Refs. [21,34]. On the other hand, our value of the C_{10} coefficient is out of the bounds estimated by Standard and Certain [21] and within the bounds of Allard *et al.* [34]. Note that the final “experimental” C_8 coefficients ($2.82\text{--}2.87 \times 10^5$ a.u.) used in Ref. [34] to construct the potential-energy curve are significantly larger than the present value, while our C_{10} lies between the experimental values ($1.16\text{--}1.34 \times 10^7$ a.u.). Since the experimental data are not very sensitive to these constants, they should be considered as effective.

B. s -wave scattering length

The s -wave scattering lengths determined from various potential-energy curves of the ground-state calcium dimer are reported in Table I. An inspection of this table shows that

TABLE III. Long-range dispersion coefficients (in a.u.) for the ground state of the calcium dimer. Numbers in parentheses represent the powers of ten.

	C_6	C_8	C_{10}
SAPT-nonrelativistic	2279.0	2.42050(5)	1.2529320(7)
SAPT-relativistic	2237.0	2.38433(5)	1.2242098(7)
Ref. [20]	2005.0	2.000(5)	1.950(7)
Ref. [21]	2740.0–2830.0	1.9(5)–2.49(5)	1.77(7)–2.28(7)
Ref. [22]	2042.0		
Ref. [23]	2325.0		
Ref. [24]	2221.0		
Experiment, Ref. [28]	2386.0		
Experiment, Ref. [34]	2081.0	2.3(5)–3.3(5)	0.4(7)–2.2(7)

this quantity is extremely sensitive to the long-range tail of the potential. Indeed, the nonrelativistic SAPT potential gives a large negative scattering length, while for the relativistic SAPT potential the sign of the scattering length changes and becomes positive. Finally, the retardation of the dipole-dipole dispersion term introduces a minor change in the scattering length. We recall here that the relativistic correction does not change the number of bound vibrational states of the ground-state potential for $J=0$, and changes the dissociation energy by 1.1%. The RKR potential obtained by inversion of the spectroscopic data of Vidal [28] also gives a negative scattering length, but the RKR curve corrected for the long range with their C_6 dispersion coefficient gives a scattering length close to the relativistic SAPT value.

Comparison of the theoretical scattering length with the value derived from the most recent experiment [34] is less satisfactory. Although the signs of the theoretical and “experimental” scattering lengths agree, the value derived from the experimental data is at least six times larger than the theoretical prediction. This disagreement can partly be explained by the difference between the theoretical and fitted C_6 coefficients, and also by the neglect of the short-range contributions at large distances.

In our opinion, the current accuracy of the relativistic ground-state potential of Ca_2 in the long range, from the present calculations and from the analysis of the most recent experimental data [33,34], allows a reliable determination of the sign of the scattering length, but not of its absolute value. Given the fact that both the present theory and the most recent experiments give a positive scattering length, we conclude that similarly to magnesium [74] it should be possible to obtain a stable Bose-Einstein condensate of calcium.

C. Potential-energy curve and spectroscopic characteristics of the $(1) {}^1\Pi_g(4s3d)$ state

The excited $(1) {}^1\Pi_g(4s3d)$ state dissociating into $\text{Ca}(^1S) + \text{Ca}(^1D)$ was not observed in any experiments, and to the best of our knowledge in the present paper we report on the very first *ab initio* study of this state. The corresponding potential-energy curve is presented in Fig. 1, while its most important spectroscopic characteristics are given in Table I. An inspection of this table shows that the $(1) {}^1\Pi_g(4s3d)$ state is strongly bound with a binding energy $D_e = 15\,127\text{ cm}^{-1}$, almost a factor of 15 larger than the binding energy of the ground state. The equilibrium distance corresponding to the minimum of the potential is $R_e = 6.39$ bohrs, also significantly smaller than for the ground state. The $(1) {}^1\Pi_g$ state has a dissociation energy $D_0 = 15\,048\text{ cm}^{-1}$, and as much as $N_v = 157$ bound vibrational levels for $J=0$.

As discussed above, compared to the ground state, the minimum of the $(1) {}^1\Pi_g$ state is shifted towards smaller distances by almost 2 bohrs, so at first glance it may seem that the transitions between these two states are not favorable due to small Franck-Condon factors. This question will be addressed in more detail in the following section. Let us stress here that these transitions will be governed by the magnitude of the magnetic transition dipole moment. The magnetic transition dipole moment M as a function of R is presented in

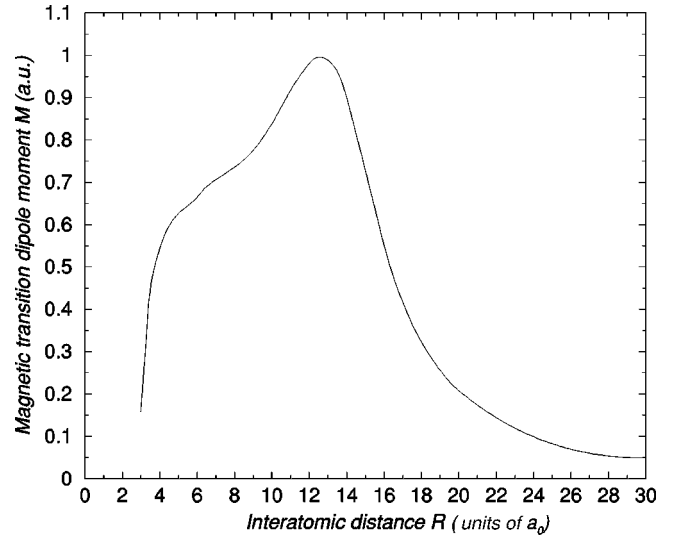


FIG. 2. Magnetic transition dipole moment (in a.u.) for the ${}^1\Pi_g \leftarrow X {}^1\Sigma_g^+$ transitions.

Fig. 2. An inspection of this figure shows that $M(R)$ is one order of magnitude smaller than a typical electric dipole function for a nonpolar van der Waals complex. This means that the intensities will be two orders of magnitude weaker than for the electric dipole-allowed transitions. However, at very low temperatures, of the order of a few mK, the level of noise in the recorded spectra should strongly be reduced compared to a few K temperature in standard molecular beams, so these transitions should be observable. Note that $M(R)$ has a maximum around $R=13$ bohrs. This suggests that the transitions between the $X {}^1\Sigma_g^+$ state and the $(1) {}^1\Pi_g$ state will be observed for high values of the excited state vibrational quantum number v' . On the other hand, the maximum of $M(R)$ is relatively broad, and the values of $M(R)$ around the minima of the ground- and excited-state potentials are still non-negligible, so other transitions should be observable as well.

D. Formation of cold calcium molecules by photoassociation spectroscopy to the excited $(1) {}^1\Pi_g(4s3d)$ state and spontaneous emission to the ground state

Having discussed the potential-energy curves for the ground $X {}^1\Sigma_g^+$ and excited $(1) {}^1\Pi_g(4s3d)$ states, and the dipole function connecting these states, we can now turn to the calculations of the photoassociation intensities probing the formation of Ca_2 in the $(1) {}^1\Pi_g$ state from the colliding ground-state calcium atoms. In our calculations, we assumed that the temperature T is the same as in the previous photoassociation experiments for Ca_2 [9], i.e., $T \approx 3$ mK. We follow Ref. [72] and assume that at this temperature mostly the s -wave interatomic collisions occur, so in the calculations of the photoassociation intensities we can limit the summation over the initial (J'') and final (J') rotational states of the calcium dimer to $J''=0$ and $J'=1$. The computed photoassociation spectrum of colliding ultracold calcium atoms to the first $(1) {}^1\Pi_g$ state as a function of the detuning frequency Δ is presented in Fig. 3. (The detuning frequency Δ is de-

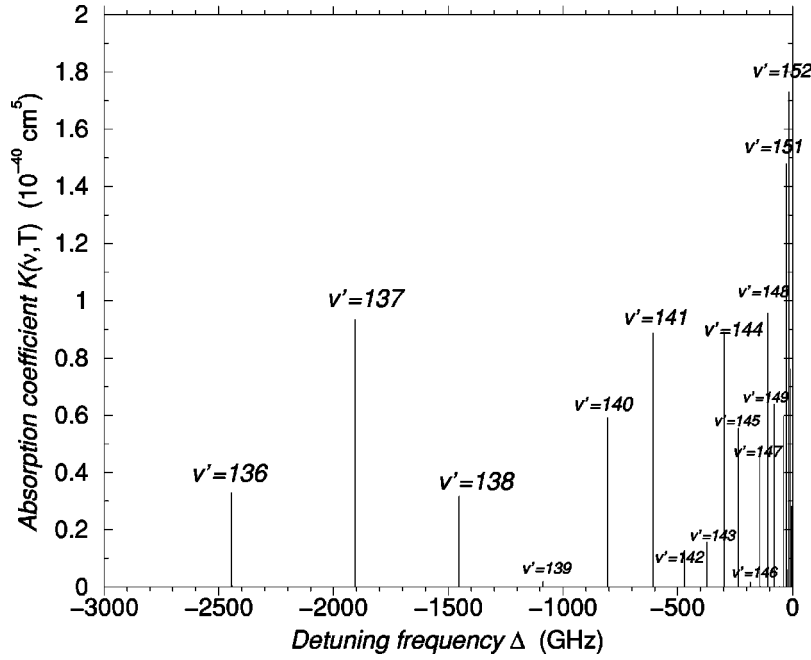


FIG. 3. Photoassociation spectrum to the $(1) {}^1\Pi_g$ state of Ca_2 at $T=3$ mK. The detuning frequency Δ is in GHz, and the intensities (for unit gas densities) in cm^5 .

defined as $\Delta = \nu - \nu_0$, where $h\nu_0$ is the energy difference between the atomic dissociation limits of the excited and ground states, $21\,849.634\text{ cm}^{-1}$ [75].) An inspection of this figure shows that the photoassociation spectrum reveals several intense transitions for detuning frequencies up to -3000 GHz. This frequency range corresponds to vibrational levels of the $J'=1$ state of Ca_2 lying between $v'=136$ and 156 . The two most intense peaks in the spectrum correspond to transitions to the vibrational states $v'=151$ and $v'=152$. Although other transitions have very small intensities ($v'=139, 142, 143, 146, \dots$), a few of them are only a third less intense than the $v'=151$ and $v'=152$ transitions (i.e., $v'=137, 141, 144, 148, \dots$) (cf. Fig. 3 and Table IV). It is interesting to observe that the photoassociation transitions appear in Fig. 3 as structureless peaks. However, each peak has its own width. For the photoassociation to the $(1) {}^1\Pi_g$ state, the predicted structure of the spectral lines is very sharp with typical widths of the order of 50 MHz.

The pumping scheme leading to the production of cold calcium molecules, as briefly discussed in Sec. II F, relies on the spontaneous emission from a bound vibrational level v' of the excited electronic state to a bound vibrational state v'' of the ground electronic state. However, the absorption process followed by a spontaneous decay mostly ends in the vibrational continuum of the ground electronic state, and only a fraction of the decay ends in the highest vibrational levels of the ground $X {}^1\Sigma_g^+$ state. The probability of these events can be estimated from the analysis of the Franck-Condon factors (cf. Sec. II F). The computed Franck-Condon factor $p_{v'}$ as a function of the vibrational quantum number v' is presented in Fig. 4. An inspection of this figure shows that $p_{v'}$ has a very sharp maximum for v' lying between 130 and 150. Thus, for the vibrational levels $v'=130-150$, the fraction of the transitions decaying to the vibrational continuum, $q_{v'} = 1 - p_{v'}$, will be small, of the order of 30–60%, suggesting that the cooling via these levels of the

$(1) {}^1\Pi_g$ state should be rather efficient. Indeed, by photoassociation we mostly populate the levels with v' ranging from $v'=136$ to 156 . Figure 4 shows that for levels with v' ranging from 136 to 146 levels as much as 42% (for $v'=136$) to 73% (for $v'=141$) of the radiative decay ends up in a discrete level of the ground electronic state (cf. Table IV). For vibrational levels with $v' > 146$, the Franck-Condon factor becomes very small. This means that even though the vibrational levels with $v' > 146$ have appreciable photoassociation intensities, they will mostly decay to the vibrational continuum of the electronic ground state. Note that for lithium

TABLE IV. Photoassociation intensities $K_{v'}$ for unit densities (in 10^{-40} cm^5), spontaneous emission coefficients $A_{v'}$ (in s^{-1}), Franck-Condon factors $p_{v'}$, and branching ratios $P(v'' \leftarrow v')$ (in %) for the transitions $X {}^1\Sigma_g^+(v'') \leftarrow {}^1\Pi_g(v')$ and for selected vibrational levels of the electronic ground and excited states of Ca_2 .

	$v'=136$	$v'=137$	$v'=138$	$v'=140$	$v'=141$
$K_{v'}^a$	0.33	0.93	0.32	0.59	0.89
$A_{v'}$	306.1	299.1	292.8	234.8	199.4
$p_{v'}$	0.42	0.45	0.50	0.61	0.71
$P(v''=31 \leftarrow v')$	29.0	8.8	0.9	0.0	0.0
$P(v''=32 \leftarrow v')$	42.2	46.6	18.8	0.0	0.0
$P(v''=33 \leftarrow v')$	1.1	17.7	53.6	3.2	0.0
$P(v''=34 \leftarrow v')$	9.8	16.0	0.3	50.0	2.9
$P(v''=35 \leftarrow v')$	10.3	0.4	13.5	26.6	59.8
$P(v''=36 \leftarrow v')$	3.7	1.8	9.1	17.0	11.1
$P(v''=37 \leftarrow v')$	0.7	3.4	2.9	3.0	15.3

^aThe quantity $K_{v'}$ represents the photoassociation intensity at a laser frequency corresponding to the vibrational level v' . The photoassociation rates $k_{v'}$ (in s^{-1}) can be obtained from the intensities by multiplying $K_{v'}$ by the gas number density n and the laser flux ϕ , while the corresponding laser power is given by the product of the photoassociation rate $k_{v'}$ and the photon energy $h\nu$.

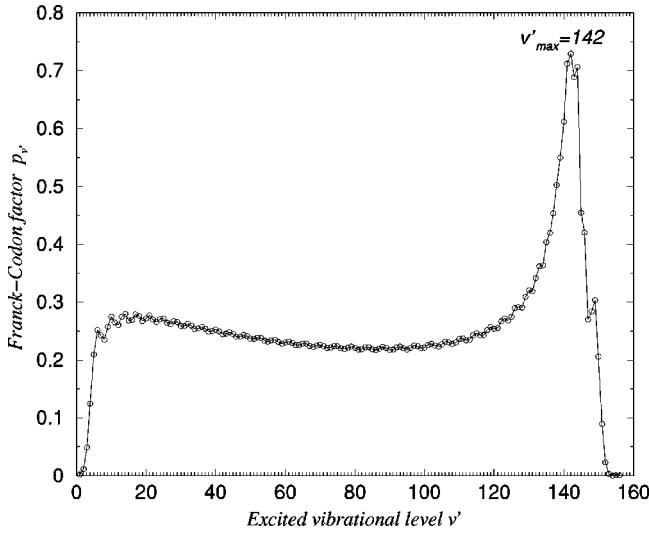


FIG. 4. Franck-Condon factors $p_{v'}$ for the $X^1\Sigma_g^+ \leftarrow (1)^1\Pi_g$ transitions.

the rate of the radiative decay to a bound vibrational level of the ground electronic state was found to be less than 1% for any vibrational level v' excited by photoassociation [72].

A better description of the spontaneous decay to the bound vibrational levels of the ground electronic state is given by the spontaneous emission coefficient, cf. Eq. (35). The spontaneous emission coefficient for the magnetic transition dipole from a vibrational state v' of the $(1)^1\Pi_g$ state to any vibrational level v'' of the ground $X^1\Sigma_g^+$ state as function of the vibrational quantum number v' is given by the sum

$$A_{v'} = \sum_{v''} A_{v'v''}. \quad (37)$$

The values of $A_{v'}$ are presented in Fig. 5. An inspection of this figure shows that the (discrete) function $A_{v'}$ for bound-to-bound transitions has a sharp maximum around $v' =$

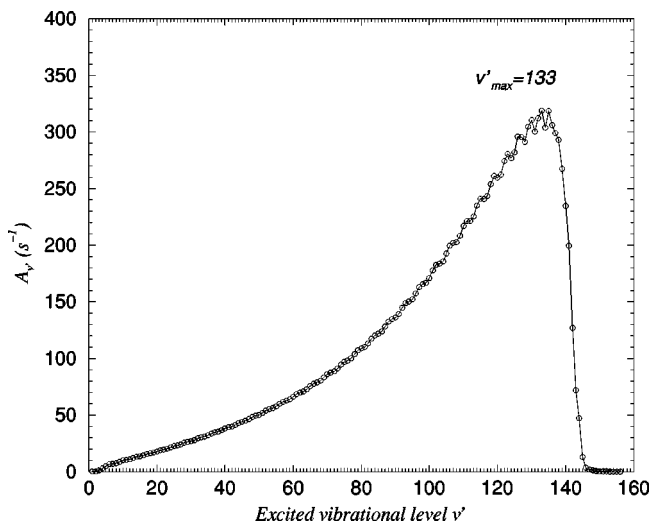


FIG. 5. Spontaneous emission coefficients $A_{v'}$ (in s^{-1}) for the $X^1\Sigma_g^+ \leftarrow (1)^1\Pi_g$ transitions.

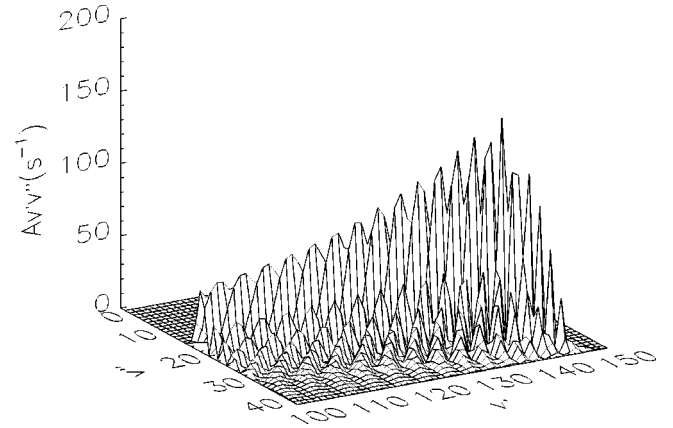


FIG. 6. Spontaneous emission coefficients $A_{v'v''}$ (in s^{-1}) for the $X^1\Sigma_g^+(v'') \leftarrow (1)^1\Pi_g(v')$ transitions.

$=133$. (Note that the maximum of the Franck-Condon factor $p_{v'}$ occurs for $v'=142$, so the magnetic transition dipole moment modifies the transition probabilities.) This means that the spontaneous emission from the vibrational level $v'=133$ ends, with the highest probability, in a bound vibrational level of the electronic ground state. However, for the vibrational levels with quantum numbers ranging from $v'=136$ to 141 , this coefficient is still very large, suggesting a large probability of spontaneous emission to bound vibrational levels of the ground electronic state of Ca_2 , while for $v' > 145$ it becomes negligible. This supports our earlier conclusion that the photoexcitation of two colliding cold calcium atoms will lead, by spontaneous emission, to the formation of calcium molecules in the ground electronic state.

In order to find how narrow is the distribution of the ground-state molecules among the vibrational levels v'' , we will analyze the state-to-state spontaneous emission coefficient defined by Eq. (35). The spontaneous emission coefficient as a function of the vibrational quantum numbers v'' and v' of the ground and excited electronic states, respectively, is presented in Fig. 6. An inspection of this figure shows that the molecules formed by spontaneous emission from the excited $(1)^1\Pi_g$ state will be in the vibrational states of the electronic ground-state with quantum numbers ranging from $v''=30$ to 37 . A more detailed view of the formation process of the ground-state Ca_2 molecules is given by the branching ratios $P(v'' \leftarrow v')$ corresponding to the spontaneous emission from a vibrational level v' to v'' :

$$P(v'' \leftarrow v') = \frac{A_{v'v''}}{\sum_{v''} A_{v'v''}} = \frac{A_{v'v''}}{A_{v'}}. \quad (38)$$

The branching ratios for the transitions $X^1\Sigma_g^+(v'') \leftarrow (1)^1\Pi_g(v')$ with $v'=136, 137, 138, 140, 141$ and $v''=31-37$ are reported in Table IV and Fig. 7. An inspection of Table IV shows that for all the initial vibrational levels v' and for one selected v'' the branching ratios are quite important, typically between 40% and 60%. Moreover, except for $v'=136$ the sum of the branching ratios over these selected vibrational levels v'' is well over 80%. Hence, the spontane-

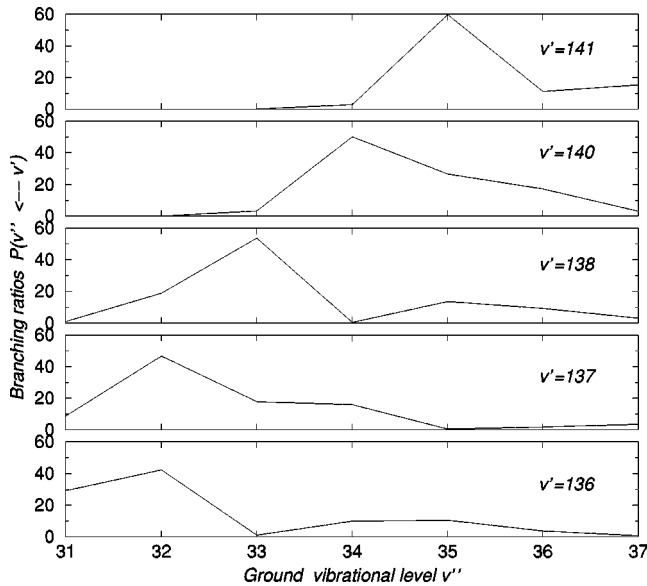


FIG. 7. Branching ratios $P(v'' \leftarrow v')$ for selected $X^1\Sigma_g^+(v'') \leftarrow {}^1\Pi_g(v')$ transitions.

ous emission from the vibrational levels v' mostly populated by the photoassociation of the ground-state atoms will lead to a narrow distribution of the vibrational levels v'' of the molecules in their ground electronic states. This means that these molecules will be very cold. Our theoretical data concerning the photoassociation intensities, Franck-Condon factors, spontaneous emission coefficients, and branching ratios suggest that the cooling scheme studied in the present paper should be efficient.

IV. SUMMARY AND CONCLUSIONS

In this paper, we have reported on a theoretical study of the ground and first excited ${}^1\Pi_g$ states of the calcium dimer and of the collisional cooling process by photoassociation spectroscopy to the $(1) {}^1\Pi_g(4s3d)$ state followed by the spontaneous emission to the ground $X^1\Sigma_g^+$ state. Our results can be summarized as follows:

(1) The *ab initio* SAPT potential for the ground state of the calcium dimer including the relativistic and QED corrections predicts the correct dissociation energy and the right sign of the scattering length. On the basis of the present calculations and of the experimental data from Tiemann and co-workers [33,34], one can conclude that it should be pos-

sible to obtain a stable Bose-Einstein condensate of calcium atoms.

(2) The computed photoassociation spectrum of colliding ultracold calcium atoms to the first ${}^1\Pi_g$ state shows several intense transitions in the detuning frequency range of up to -3000 GHz. This frequency range corresponds to vibrational levels of the $J'=1$ state of Ca_2 ranging from $v'=136$ to 156 with a maximum for $v'=152$.

(3) The spontaneous emission coefficient from a vibrational state v' of the $(1) {}^1\Pi_g$ state to any vibrational level of the ground $X^1\Sigma_g^+$ state shows a sharp maximum around $v'=133$. However, for the levels with v' ranging from 136 to 141 this coefficient is still very large, suggesting a large probability of spontaneous emission to a vibrational level of the ground electronic state of Ca_2 . Thus, the photoexcitation of two colliding cold calcium atoms will lead, by spontaneous emission, to the formation of cold calcium molecules.

(4) A more detailed analysis of the spontaneous emission coefficient and of the branching ratios as a function of the vibrational quantum numbers v'' and v' of the ground and excited electronic states, respectively, suggests that the molecules formed by spontaneous emission from the excited $(1) {}^1\Pi_g$ state will be in the vibrational states v'' ranging from 30 to 37 . Such a narrow vibrational distribution will lead to vibrationally cold molecules.

(5) The computed Franck-Condon factors ($p_{v'}$) show a very sharp maximum for v' ranging from 130 to 150 . Thus, for the vibrational levels with $v'=130-150$, the fraction of the transitions that terminate in the continuum ($q_{v'}=1-p_{v'}$) will be small ($30-60\%$), suggesting that the cooling via these levels of the $(1) {}^1\Pi_g$ state should be rather efficient.

As a next step of this study, we plan to investigate the collisional cooling of Ca_2 via the first ${}^3\Pi_u$ state dissociating into $\text{Ca}(^1S)+\text{Ca}(^3P)$ and the vibrational relaxation mechanisms induced by inelastic $\text{Ca}+\text{Ca}_2$ collisions. Works in this direction are in progress.

ACKNOWLEDGMENTS

We would like to thank Professor Bogumil Jeziorski, Professor Eberhard Tiemann, and Dr. Asen Pashov for many useful discussions and for reading and commenting on the manuscript. We also thank Professor Michal Jaszunski for his invaluable help with the DALTON program. This work was supported by the Polish Scientific Research Council (KBN) within Grant No. 4 T09A 071 22.

[1] F. Dalfovo, S. Giorgini, L.P. Pitaevskii, and S. Stringari, *Rev. Mod. Phys.* **71**, 463 (1999).
 [2] J. Weiner, V.S. Bagnato, S. Zilio, and P.S. Julienne, *Rev. Mod. Phys.* **71**, 1 (1999).
 [3] K. Sengstock, U. Sterr, G. Hennig, D. Bettermann, J.H. Müller, and W. Ertmer, *Opt. Commun.* **103**, 73 (1993).
 [4] T. Kurosu and F. Shimizu, *Jpn. J. Appl. Phys., Part 2* **29**, L2127 (1990).

[5] T. Binnewies, G. Wilpers, U. Sterr, F. Riehle, J. Helmcke, T.E. Mehlstäubler, E.M. Rasel, and W. Ertmer, *Phys. Rev. Lett.* **87**, 123002 (2001).
 [6] H. Katori, T. Ido, Y. Isoya, and M. Kuwata-Gonokami, *Phys. Rev. Lett.* **82**, 1116 (1999).
 [7] T. Ido, Y. Isoya, and H. Katori, *Phys. Rev. A* **61**, 061403(R) (2000).
 [8] T.P. Dinneen, K.R. Vogel, E. Arimondo, J.L. Hall, and A. Gal-

- lagher, Phys. Rev. A **59**, 1216 (1999).
- [9] G. Zinner, T. Binnewies, F. Riehle, and E. Tiemann, Phys. Rev. Lett. **85**, 2292 (2000).
- [10] M. Machholm, P.S. Julienne, and K.-A. Suominen, Phys. Rev. A **59**, R4113 (1999).
- [11] M. Machholm, P.S. Julienne, and K.-A. Suominen, Phys. Rev. A **64**, 033425 (2001).
- [12] M. Machholm, P.S. Julienne, and K.-A. Suominen, Phys. Rev. A **65**, 023401 (2002).
- [13] E. Tiemann, in Proceedings of the Conference on Cold Molecules, Gif-sur-Yvette, France, 2001 (unpublished).
- [14] R.O. Jones, J. Chem. Phys. **71**, 1300 (1979).
- [15] M.E. Rosenkrantz, M. Krauss, and W.J. Stevens, Chem. Phys. Lett. **89**, 4 (1982).
- [16] K.G. Dyall and A.D. McLean, J. Chem. Phys. **97**, 8424 (1992).
- [17] J.W. Mirick, C.-H. Chien, and E. Baisten-Barojas, Phys. Rev. A **63**, 023202 (2001).
- [18] J.M. Peréz-Jordá and A.D. Becke, Chem. Phys. Lett. **233**, 134 (1995).
- [19] A. Milet, T. Korona, R. Moszynski, and E. Kochanski, J. Chem. Phys. **111**, 7727 (1999).
- [20] F. Maeder and W. Kutzelnigg, Chem. Phys. Lett. **42**, 95 (1979).
- [21] J.M. Standard and P.R. Certain, J. Chem. Phys. **83**, 3002 (1985).
- [22] J.F. Stanton, Phys. Rev. A **49**, 1698 (1994).
- [23] M. Mérawa, C. Tendero, and M. Rérat, Chem. Phys. Lett. **343**, 397 (2001).
- [24] S.G. Porsev and A. Derevianko, Phys. Rev. A **65**, 020701(R) (2002).
- [25] W.J. Balfour and R.F. Whitlock, Can. J. Phys. **53**, 472 (1975).
- [26] K. Sakurai and H.P. Broida, J. Chem. Phys. **65**, 1138 (1976).
- [27] J.C. Wyss, J. Chem. Phys. **71**, 2949 (1979).
- [28] C.R. Vidal, J. Chem. Phys. **72**, 1864 (1980).
- [29] V.F. Bondybey and J.H. English, Chem. Phys. Lett. **111**, 195 (1984).
- [30] R.T. Hofmann and D.O. Harris, J. Chem. Phys. **85**, 3749 (1986).
- [31] M.A. Gondal, M.A. Khan, and M.H. Rais, Chem. Phys. Lett. **243**, 94 (1995).
- [32] M.A. Gondal, M.A. Khan, and M.H. Rais, Nuovo Cimento D **20**, 723 (1998).
- [33] O. Allard, A. Pashov, H. Knöckel, and E. Tiemann, Phys. Rev. A **66**, 042503 (2002).
- [34] O. Allard, C. Samuelis, A. Pashov, H. Knöckel, and E. Tiemann, Eur. Phys. J. D (to be published).
- [35] J.C. Miller, B.S. Ault, and L. Andrews, J. Chem. Phys. **67**, 2478 (1977).
- [36] L. Andrews, W.W. Duley, and L. Brewer, J. Mater. Sci. Technol. **70**, 41 (1978).
- [37] J.C. Miller and L. Andrews, J. Chem. Phys. **68**, 1701 (1978).
- [38] J.C. Miller and L. Andrews, J. Chem. Phys. **69**, 2054 (1978).
- [39] M.A. Gaveau, M. Briant, P.R. Fournier, J.M. Mestdagh, and J.P. Visticot, J. Chem. Phys. **116**, 955 (2002).
- [40] B. Jeziorski, R. Moszynski, and K. Szalewicz, Chem. Rev. **94**, 1887 (1994).
- [41] R. Moszynski, P.E.S. Wormer, and A. van der Avoird, in *Computational Molecular Spectroscopy*, edited by P.R. Bunker and P. Jensen (Wiley, New York, 2000), p. 69.
- [42] T. Korona, R. Moszynski, F. Thibault, J.-M. Launay, B. Bussery-Honvault, J. Boisssoles, and P.E.S. Wormer, J. Chem. Phys. **115**, 3074 (2001).
- [43] R. Moszynski, B. Jeziorski, A. Ratkiewicz, and S. Rybak, J. Chem. Phys. **99**, 8856 (1993).
- [44] R. Moszynski, S.M. Cybulski, and G. Chalasinski, J. Chem. Phys. **100**, 4998 (1994).
- [45] R. Moszynski, B. Jeziorski, and K. Szalewicz, J. Chem. Phys. **100**, 1312 (1994).
- [46] R. Moszynski, S. Rybak, B. Jeziorski, K. Szalewicz, and H.L. Williams, J. Chem. Phys. **100**, 5080 (1994).
- [47] S. Rybak, B. Jeziorski, and K. Szalewicz, J. Chem. Phys. **95**, 6576 (1991).
- [48] G. Chalasinski and B. Jeziorski, Theor. Chim. Acta **46**, 277 (1977).
- [49] M. Jeziorska, B. Jeziorski, and J. Cizek, Int. J. Quantum Chem. **32**, 149 (1987).
- [50] R. Moszynski, T.G.A. Heijmen, and B. Jeziorski, Mol. Phys. **88**, 741 (1996).
- [51] R.J. Bemish, L. Oudejans, R.E. Miller, R. Moszynski, T.G.A. Heijmen, T. Korona, P.E.S. Wormer, and A. van der Avoird, J. Chem. Phys. **109**, 8968 (1998).
- [52] B. Jeziorski, R. Moszynski, A. Ratkiewicz, S. Rybak, K. Szalewicz, and H.L. Williams, in *Methods and Techniques in Computational Chemistry: METECC94*, edited by E. Clementi (STEF, Cagliari, 1993), Vol. B, p. 79.
- [53] A.J. Sadlej, M. Urban, and O. Gropen, Phys. Rev. A **44**, 5547 (1991).
- [54] R. Moszynski, P.E.S. Wormer, B. Jeziorski, and A. van der Avoird, J. Chem. Phys. **101**, 2811 (1994).
- [55] K.T. Tang and J.P. Toennies, J. Chem. Phys. **80**, 3726 (1984).
- [56] P.E.S. Wormer and H. Hettema, J. Chem. Phys. **97**, 5592 (1992).
- [57] P.E.S. Wormer and H. Hettema, computer code POLCOR package (University of Nijmegen, The Netherlands, 1992).
- [58] H.A. Bethe and E.E. Salpeter, *Quantum Mechanics of One- and Two-Electron Atoms* (Academic Press, New York, 1957), p. 170.
- [59] W.J. Meath and J.O. Hirschfelder, J. Chem. Phys. **44**, 3197 (1966).
- [60] W.J. Meath and J.O. Hirschfelder, J. Chem. Phys. **44**, 3210 (1966).
- [61] J.O. Hirschfelder and W.J. Meath, Adv. Chem. Phys. **12**, 1 (1967).
- [62] R. Moszynski, G. Lach, M. Jaszunski, and B. Bussery-Honvault, Phys. Rev. A (to be published).
- [63] R.D. Cowan and D.C. Griffin, J. Opt. Soc. Am. **66**, 1010 (1976).
- [64] K. Andersson, M.C. Barysz, A. Bernhardsson, M.R.A. Blomberg, D.L. Cooper, T. Fleig, M.P. Fülscher, Coen de Graaf, B. Hess, G. Karlström, R. Lindh, P.-Å. Malmqvist, P. Neogrády, J. Olsen, B.O. Roos, A.J. Sadlej, M. Schütz, B. Schimmelpfennig, L. Seijo, L. Serrano-Andrés, P.E.M. Siegbahn, J. Stålring, T. Thorsteinsson, V. Veryazov, M. Wierzbowska, and P.-O. Widmark, computer code MOLCAS version 5.0 (Lund University, Sweden, 2001).
- [65] H.B.G. Casimir and D. Polder, Phys. Rev. **73**, 360 (1948).
- [66] H. Koch and P. Jørgensen, J. Chem. Phys. **93**, 3333 (1990).
- [67] T. Helgaker, H.J. Aa. Jensen, P. Jørgensen, J. Olsen, K. Ruud,

- H. Ågren, A.A. Auer, K.L. Bak, V. Bakken, O. Christiansen, S. Coriani, P. Dahle, E.K. Dalskov, T. Enevoldsen, B. Fernandez, C. Hättig, K. Hald, A. Halkier, H. Heiberg, H. Hettema, D. Jonsson, S. Kirpekar, R. Kobayashi, H. Koch, K.V. Mikkelsen, P. Norman, M.J. Packer, T.B. Pedersen, T.A. Ruden, A. Sanchez, T. Saue, S.P.A. Sauer, B. Schimmelpfenning, K.O. Sylvester-Hvid, P.R. Taylor, and O. Vahtras, computer code DALTON, an *ab initio* electronic structure program, Release 1.2, 2001.
- [68] S.F. Boys and F. Bernardi, *Mol. Phys.* **19**, 553 (1970).
- [69] P.R. Bunker and P. Jensen, *Molecular Symmetry and Spectroscopy* (Academic, Ottawa, 1998).
- [70] G. Herzberg, *Molecular Spectra and Molecular Structure. I. Spectra of Diatomic Molecules* (Van Nostrand, New York, 1950).
- [71] H.R. Thorsheim, J. Weiner, and P.S. Julienne, *Phys. Rev. Lett.* **58**, 2420 (1987).
- [72] R. Côté and A. Dalgarno, *Phys. Rev. A* **58**, 498 (1998).
- [73] R. Côté and A. Dalgarno, *J. Mol. Spectrosc.* **195**, 236 (1999).
- [74] E. Tiesinga, S. Kotochigova, and P.S. Julienne, *Phys. Rev. A* **65**, 042722 (2002).
- [75] For the atomic data for the calcium atom see the National Institute of Standards and Technology web site at <http://www.physics.nist.gov/PhysRefData>